Published in final edited form as:
Biol Cell. 2009 March ; 101(3): 133–140. doi:10.1042/BC20080083.

Osteoclast differentiation and function in aquaglyceroporin AQP9 null mice

Yangjian Liu[1,2], **Linhua Song**[1], **Yiding Wang**[1], **Aleksandra Rojek**[3], **Søren Nielsen**[3], **Peter Agre**[1,4], and **Jennifer M. Carbrey**[1]

[1]From Department of Cell Biology, Duke University Medical Center, Durham, NC 27710, USA

[2]Department of Biological Chemistry, The Johns Hopkins University School of Medicine, Baltimore, MD 21205, USA

[3]Water and Salt Research Center, University of Aarhus, DK-8000 Aarhus, Denmark

[4]Department of Molecular Microbiology and Immunology and Malaria Research Institute, The Johns Hopkins Bloomberg School of Public Health, Baltimore, MD 21205, USA

Abstract

Background Information—Osteoclasts are cells specialized for bone resorption and play important roles in bone growth and calcium homeostasis. Differentiation of osteoclasts involves fusion of bone marrow macrophage mononuclear precursors in response to extracellular signals. A dramatic increase in osteoclast cell volume occurs during osteoclast biogenesis and is believed to be mediated by Aquaporin 9 (AQP9), a membrane protein that can rapidly transport water and other small neutral solutes across cell membranes.

Results—Here we report an increase in expression of AQP9 during differentiation of a mouse macrophage cell line into osteoclasts. Bone marrow macrophages from wild type and AQP9 null mice differentiate into osteoclasts that have similar morphology, contain comparable numbers of nuclei, and digest synthetic bone to the same extent. Bones from wild type and AQP9 null mice contain similar numbers of osteoclasts and have comparable density and structure as measured by X-ray absorptiometry and micro-computed tomography.

Conclusions—Our data confirm that AQP9 expression rises during osteoclast biogenesis but indicate that AQP9 is not essential for osteoclast function or differentiation under normal physiological conditions.

Keywords

aquaporin; aquaglyceroporin; osteoclast; bone; AQP9

Address correspondence to: Jennifer M. Carbrey, Ph.D., Department of Cell Biology, Duke Medical Center, Box 102143, Durham, NC 27710; Phone 919-681-4931; Fax 919-684-8793; E-mail: carbr001@mc.duke.edu.

INTRODUCTION

Dynamic bone remodeling is essential for bone growth and calcium homeostasis. An imbalance in bone remodeling with excessive bone resorption by osteoclasts in comparison to formation by osteoblasts is associated with osteoporosis, an endemic disease characterized by low bone density and fragile bones (Teitelbaum, 2000). While osteoblasts are derived from mesenchyme, osteoclasts are differentiated from the monocyte-macrophage lineage. Macrophage precursors fuse with each other and differentiate into multi-nucleated osteoclasts when stimulated by M-CSF (macrophage colony stimulating factor) (Udagawa et al., 1990) and RANKL (receptor activator of NF-κB ligand) (Lacey et al., 1998), a member of the tumor necrosis factor family expressed by osteoblasts. The differentiated osteoclasts attach to bones and polarize to acidify the contact area between the cell and the bone for solubilization (Baron et al., 1985). Osteoclasts also secrete the protease cathepsin K (Cath K) to digest the organic component of bone (Drake et al., 1996). The degradation products are taken up and released at the antiresorptive surface of osteoclasts by transcytosis (Nesbitt and Horton, 1997).

To maximize bone resorption, osteoclasts expand surface area by fusion of many mononucleated macrophages (Vignery, 2000). The mechanism behind the increase in surface area during cell fusion is important for understanding osteoclast biogenesis and the pathophysiological function of osteoclasts. One model hypothesizes that the volume of an osteoclast is greater than the sum of its precursor cells which means that a large amount of water needs to be acquired during osteoclast biogenesis (Aharon and Bar-Shavit, 2006).

Aquaporins are a family of small membrane proteins that transport water and other small solutes across cell membranes. Aquaporins are widely expressed in many tissues and play fundamental roles in regulating body fluid homeostasis (Agre et al., 2002). All Aquaporins are similar in membrane topology but some differ in substrate specificity. Based on the amino acid homology and solute permeability, aquaporins can be categorized into two subfamilies: i) the aquaporin subfamily that selectively transports water and ii) the aquaglyceroporin subfamily that transports a range of small neutral solutes, including water, glycerol, and urea. Recently, Aharon and Bar-Shavit detected increased expression of Aquaporin 9 (AQP9), an aquaglyceroporin, in osteoclasts differentiated from bone marrow macrophages and proposed that AQP9 mediates large amounts of water influx that is necessary for osteoclast biogenesis (Aharon and Bar-Shavit, 2006). In this study, we used AQP9 null mice to study the role of AQP9 in osteoclast differentiation, bone resorption, and bone integrity. We confirm increased expression of AQP9 during osteoclast differentiation, however we do not detect functional defects in bone in the AQP9 null animals.

RESULTS

Expression of AQP9 in osteoclasts

Previous studies have shown that AQP9 is expressed in peripheral leukocytes (Ishibashi et al., 1998). To test if AQP9 is also expressed in osteoclasts, the membrane fractions of RAW264.7 cells and RAW264.7 cells differentiated in culture to become osteoclasts were analyzed by Western blot with a rat AQP9 antibody. A band with a molecular weight of

about 32 kDa was recognized by the rat AQP9 antibody in samples from RAW264.7 cells before and after differentiation. The expression of AQP9 increased about 4 fold after RAW264.7 cells were differentiated to osteoclasts (Fig. 1A).

To confirm the expression of AQP9 in mouse osteoclasts, bone marrow macrophages (BMMs) were isolated from wild type and AQP9 null mice and differentiated into osteoclasts. RT-PCR results revealed that AQP9 is expressed in both wild type BMMs and osteoclasts differentiated from BMMs. However, AQP9 was absent in RNA samples prepared from AQP9 null BMMs and differentiated BMMs (Fig. 1B). The deficiency of AQP9 in cells from AQP9 null mice is not compensated by the expression of AQP3 or AQP7, the two additional aquaglyceroporins known to be expressed in mouse (Fig. 1C), or any of the other mouse aquaporins (data not shown).

Differentiation of AQP9 null osteoclasts

To study whether deficiency of AQP9 affects osteoclast biogenesis, BMMs isolated from mice were induced to differentiate into osteoclasts in the presence of M-CSF and RANKL. The expression of osteoclast markers, matrix metalloproteinases 9 (MMP9) and cathepsin K (Cath K), was examined. RT-PCR results revealed that the absence of AQP9 does not affect the expression of osteoclast markers (Fig. 1B). TRAP staining showed that the morphology of AQP9 null BMM-derived osteoclasts was not different from wild type BMM-derived osteoclasts (Fig. 2A). Wild type and AQP9 null BMM-derived osteoclasts displayed similar distribution and range of surface areas and contained similar numbers of nuclei (Fig. 2B).

We next examined the role of AQP9 on the bone resorption by BMM-derived osteoclasts. BMMs isolated from both wild type and AQP9 null mice were cultured on osteologic slices and induced to differentiate into osteoclasts. Osteoclasts differentiated from both types of BMMs digested bone matrix and formed resorption pits. There was no difference in the area of resorption pits between wild type and AQP9 null BMM-derived osteoclasts (Fig. 2C).

Effect of phloretin on AQP9 null osteoclast differentiation

Recent studies by Aharon and Bar-Shavit hypothesized that AQP9 is the major water channel involved in volume regulation during osteoclast biogenesis (Aharon and Bar-Shavit, 2006). One argument in these studies was that phloretin, a pharmacological inhibitor of AQP9 as well as other channels, could efficiently block the differentiation of osteoclasts. To test this, phloretin together with M-CSF and RANKL was added to the culture media of both wild type and AQP9 null macrophages for the last two days of differentiation. In addition to causing cell death, TRAP staining revealed that phloretin affected the differentiation process of both wild type and AQP9 null macrophages into osteoclasts (Fig. 3)

Mineral density and structure of AQP9 null mice bones

Since osteoclasts play an important role in bone remodeling, we studied the effect of AQP9 on osteoclast function *in vivo*. Femurs and tibias were isolated from one year old female wild type and AQP9 null mice. There was no significant difference in bone length between wild type and AQP9 null long bones (tibias or femurs) (Fig. 4A). Histological staining revealed that the osteoclast number in AQP9 null mice bones is similar to that in the wild

type mice (Fig. 4B). Densitometric study using dual energy x-ray absorptiometry (DEXA) showed negligible density differences between wild type and AQP9 null bones of 4 month old mice (Fig. 4C) as well as mice up to 12 months old (data not shown). In addition, DEXA analysis of whole body bone density of wild type and AQP9 null mice aged 4, 6, or 10 weeks revealed similar densities (Fig. 4D). The structures of the cortical and trabecular areas of femurs were also analyzed by micro-computed tomography (μCT) and revealed that absence of AQP9 does not change the structure of the femur (Fig. 4E). Similar to the results of the densitometric study, bone volume of femurs from AQP9 null animals was not affected by the lack of the AQP9 gene (Fig. 4F).

DISCUSSION

Since the discovery of the first aquaporin water channel, twelve other aquaporins have been identified in mammals. Mutations in aquaporin genes have been shown to be associated with diseases such as cataracts, nephrogenic diabetes insipidus (NDI), and obesity (Agre et al., 2002). Numerous studies have been conducted to understand the physiological role of aquaporins in multiple tissues under normal and pathophysiological conditions. AQP9 was first identified in leukocytes (Ishibashi et al., 1998) and then shown to be expressed in liver, epididymis, testis, spleen, brain (Elkjaer et al., 2000) and recently in mouse red cells (Liu et al., 2007). When ectopically expressed in Xenopus oocytes, AQP9 transports a broad range of neutral solutes (Tsukaguchi et al., 1998). Functional studies of AQP9 in the liver have shown that AQP9 plays an important role in glycerol metabolism. The expression of AQP9 in liver is up-regulated by fasting and down-regulated by refeeding, which is hypothesized to mediate glycerol uptake for gluconeogenesis (Kuriyama et al., 2002; Carbrey et al., 2003). Blockage of the glycerol uptake pathway by disruption of AQP9 in mice leads to an increase in serum glycerol levels (Rojek et al., 2007).

Osteoclasts are resident bone macrophages that are responsible for bone matrix resorption. To increase the efficiency of bone resorption, osteoclasts dramatically expand their surface area by fusing many mononucleated macrophage precursors (Vignery, 2000). The giant mature osteoclasts attach firmly to bone matrix with a ‘sealing structure’ rich in actin and integrins, and secrete protons and proteases into the contacting area to digest the bone (Teitelbaum, 2000). Aquaporin water channels have been well known to regulate the permeability of water and other small solutes across cell membranes under many physiological processes (Agre et al., 2002). Involvement of aquaporins in regulating the volume of osteoclast precursors during osteoclast biogenesis is possible.

Studying normal mice, Aharon and Bar-Shavit (2006) recently showed that AQP9 expression is increased in BMM-derived osteoclasts. They hypothesized that AQP9 functions to regulate cell volume during osteoclast differentiation and cell fusion. When cells that were differentiating to become osteoclasts were incubated with phloretin, a non-specific inhibitor of AQP9, the surface area of the forming osteoclasts was much smaller than untreated cells (Aharon and Bar-Shavit, 2006). However, phloretin is a broad-spectrum inhibitor which can block the activity of AQP9 as well as urea transporters, chloride channels, and other channels (Knepper and Star, 1990; Fan et al., 2001; Yamaguchi and Ishikawa, 2005; Abdullaev et al., 2006). AQP9 null mice provided us an excellent resource

to define the role of AQP9 in osteoclasts. In our *in vitro* osteoclast biogenesis experiments, AQP9 null BMM-derived osteoclasts were not different from wild type BMM-derived osteoclasts in morphology, and phloretin has a similar inhibitory effect on the differentiation of both wild type and AQP9 null osteoclasts. Therefore, we feel that the results of Aharon and Bar-Shavit need to be reinterpreted in light of our studies of the AQP9 null mice.

We also detected the expression of AQP9 in the mouse pre-osteoclast macrophage cell line, RAW264.7, and observed that AQP9 expression increased during the differentiation of RAW264.7 cells into osteoclasts in culture. With AQP9 null mice, we confirmed that AQP9 expression is increased in isolated BMMs and osteoclasts differentiated from BMMs. The absence of AQP9 does not affect the differentiation or functional activity of osteoclasts. In AQP9 null osteoclasts, deficiency of AQP9 was not compensated by the expression of other members of the aquaglyceroporin subfamily. In the *in vivo* mouse system, the absence of AQP9 did not affect the bone density, bone mass or bone integrity. Our data indicate that AQP9 is not essential for osteoclasts under physiological conditions. This may be explained if the diffusion across the bilayer of water, or another solute that AQP9 transports, is adequate under normal situations. It is possible that AQP9 may become important when osteoclasts are stressed.

The water permeability of AQP9 is relatively low compared to other classic aquaporins, such as AQP4 (Carbrey et al., 2003). It is more likely that osteoclasts would express an aquaporin other than AQP9 if rapid water influx is needed during osteoclast biogenesis. Of known AQP9 transport substrates (Tsukaguchi et al., 1998), none of them except water has been shown to be utilized by osteoclasts physiologically. To define the role of AQP9 in osteoclasts, further investigations will involve identifying the AQP9 transport substrate in osteoclasts and studying bone phenotypes of AQP9 null animals under different stress conditions.

MATERIALS AND METHODS

Animal studies

AQP9 null mice were generated by targeted gene disruption as described (Rojek et al., 2007) and backcrossed to mouse strain C57L/B6 for a homogeneous genetic background. Under physiological conditions, these mice have normal embryonic survival, growth, fertility, appearance, behavior, and plasma parameters except for a significant increase in the level of glycerol and triglycerides. Mouse genotyping was performed by PCR as described (Rojek et al., 2007). Animal protocols were approved by Institutional Animal Care and Use Committees at The Johns Hopkins University and Duke University.

Cell culture of RAW264.7

The murine pre-osteoclast macrophage cell line, RAW264.7, was obtained from ATCC (Manassas, VA). RAW264.7 cells were cultured in DMEM (Cellgro, Kansas City, MO) containing 4.5g/L glucose and supplemented with 10% heat-inactivated FBS (Sigma, St. Louis, MO) and 0.5 units/ml penicillin, 50 μg/ml streptomycin (Cellgro, Kansas City, MO).

Isolation and purification of mouse BMMs

Mouse long bones were isolated from adult wild type and AQP9 null mice in a sterile environment. Bone marrow cells were flushed from bones with α-MEM (Gibco, Carlsbad, CA) with a 22G needle and syringe. After washing once with α-MEM, cells were resuspended and plated in a 150 mm petri dish in α-MEM supplemented with 10% heat-inactivated FBS and 50 ng/ml M-CSF (Sigma, St. Louis, MO) for four days. The resulting attached cells were BMMs, which were removed with 0.05% trypsin (Cellgro, Kansas City, MO) and split into cell culture plates for osteoclastogenesis (Bai et al., 2005).

In vitro osteoclastogenesis

To induce osteoclast differentiation, RAW264.7 cells or isolated BMMs were plated at a density of $2.5x10^4$ cells/cm^2. 10 ng/ml of M-CSF and 50 or 100 ng/ml of RANKL (R&D system, Minneapolis, MN) were added to the culture media to induce osteoclast biogenesis. Media was changed at day 3 with fresh M-CSF and RANKL. Normally, multi-nucleated osteoclasts were observed at day 4. For phloretin inhibition experiments, 50 μM of phloretin (Sigma, St. Louis, MO) dissolved in DMSO was added to the culture media of BMMs for the last two days after three days incubation with M-CSF and RANKL.

TRAP (tartrate -resistant acid phosphatase) staining of osteoclasts

To identify osteoclasts, cells grown on coverslips were fixed with 4% paraformaldehyde in PBS (pH7.4) for 10 min, and then permeablilzed with 0.5% Triton X-100 in PBS for another 10 min. Subsequently, fixed cells on coverslips were incubated with 0.01% naphthol AS-MX phosphate (Sigma, St. Louis, MO) and 0.05% fast red violet LB salt (Sigma, St. Louis, MO) in the presence of 50 mM sodium tartrate and 90 mM sodium acetate (pH5.0) for 5 min (Hotokezaka et al., 2002). The TRAP positive cells containing more than four nuclei were considered osteoclasts. Cells were imaged with an Axiovert 200 inverted light microscope with Axiocam MRC 5 camera and Axiovision software (Carl Zeiss MicroImaging, Thornwood, NY).

In vitro bone resorption assay of osteoclasts

Isolated BMMs were plated in a 24-well BD BioCoat Osteologic Bone Cell Culture System (BD Bioscience, San Jose, CA) in the presence of 10 ng/ml M-CSF and 100 ng/ml RANKL. After 5 days, cells were removed with bleach and washed with water. The resorption pits were imaged using the same imaging system as the TRAP-stained cells described above.

Western blot

Membrane fractions of macrophages and osteoclasts were prepared by centrifugation (Carbrey et al., 2003). Immunoblotting was performed as described (Smith et al., 1994). About 30 μg of membrane protein was analyzed by 12% SDS/PAGE. Immunoblots were incubated with 3.5 μg/ml rabbit anti-rat AQP9 antibody (Alpha Diagnostic Inc., San Antonio, TX). After incubation with 1:10,000 HRP-labeled goat anti-rabbit IgG (Amersham, Arlington Heights, IL) for 1 hour at room temperature, the targeted proteins were visualized by chemiluminescence (ECL plus, Amersham, Piscataway, NJ).

RT-PCR

Total mRNA from cultured cells was isolated using RNeasy (QIAGEN, Valencia, CA). Primers for DNA synthesis were designed based on reported mouse cDNA sequences: AQP9, 5′-ATGCCTTCTGAGAAGGACCGAG-3′ and 5′-CTACATGATGACGCTGAGTTCG-3′; Cath K, 5′-AGAAGATGACGGGACTCAGAA TAC-3′ and 5′-CGTGGCGTTATACATACAACTTTC-3′; MMP9, 5′-CTTCCCTCTGAATAAAGACGACA T-3′ and 5′-CTGTAATGGGCTTCCTCTATGATT-3′; Actin, 5′-GACAGGATGCAGAAGGAGATTACT-3′ and 5′-TAGGTTTTGTCAAAGAAAGGGTGT-3′; AQP3, 5′-CTCATCCTTGTGATGTTTGGC-3′ and 5′-TGTGCCTATGAACTGATCAAA-3′; AQP7, 5′-TATGTCATGATGGTGTTTGGC-3′ and 5′-GGTTAATGGCACCATAGAAAA-3′. DNA was amplified from total mRNA (18ng) with SuperScript™ III One-Step RT-PCR System (Invitrogen, Carlsbad, CA) for 35 cycles that consisted of 94°C for 0.5 minute, 55°C for 0.5 minute, and 72°C for 1 minute. Reaction mixtures (10 μl) were analyzed by 1.0% agarose gel electrophoresis.

In vivo osteoclast analysis

After removal of soft tissue, mouse knee joints with intact tibias and femurs were fixed overnight in 4% paraformaldehyde in PBS (pH7.4), decalcified in an EDTA solution (20%, pH7.2) at room temperature for two weeks, embedded in paraffin, sectioned at a thickness of 5 μm, and stained with 0.02% naphthol AS-MX phosphate and 0.1% fast red violet LB salt in the presence of 50 mM sodium tartrate and 90 mM sodium acetate (pH5.0) for 30 min. *In vivo* osteoclast density was determined by counting osteoclasts in areas situated on the cortical side of the growth plate in tibias.

Densitometric and μCT analysis of bone mass

Femurs and tibias from the right legs of mice were harvested from male and female wild type and AQP9 null mice. Adult mice from 4-12 months old were studied as well as 4, 6, and 10 week old mice. Bone mineral density (BMD, g/cm^2) was measured using a dual energy X-ray absorptiometry (DEXA) LunarPIXIMUS2 densitometer (Lunar Corp., Madison, WI) following the manufacture's guidelines.

Femurs were also evaluated by micro-computed tomography (μCT40, Scanco Medical, Basserdorf, Switzerland) to determine their mass. Bones were scanned at 70 kEv with a cone beam in medium-resolution mode and a slice increment of 5.2 μm. 300 slices were scanned starting from the bottom of the condyles for trabecular bone and down the middle of psoas major for cortical bone. Three-dimentional reconstruction of slices was performed using μCT40 computer software. Bone volume (BV) to tissue volume (TV) representing the bone density was calculated (Wang et al., 2005).

ACKNOWLEDGEMENTS

We thank Patrick J. Flannery for his assistance with DEXA and μCT. This work was supported in part by National Institutes of Health Grant HL48268.

ABBREVIATIONS

AQP	aquaporin
RANKL	receptor activator of NF-κB ligand
M-CSF	macrophage colony stimulating factor
BMMs	bone marrow macrophages
MMP9	matrix metalloproteinases 9
Cath K	cathepsin K
DEXA	dual energy x-ray absorptiometry
μCT	micro-computed tomography
TRAP	Tartrate-Resistant Acid Phosphatase

REFERENCES

Abdullaev IF, Rudkouskaya A, Schools GP, Kimelberg HK, Mongin AA. Pharmacological comparison of swelling-activated excitatory amino acid release and Cl- currents in cultured rat astrocytes. J. Physiol. 2006; 572:677–689. [PubMed: 16527858]

Agre P, King LS, Yasui M, Guggino WB, Ottersen OP, Fujiyoshi Y, Engel A, Nielsen S. Aquaporin water channels--from atomic structure to clinical medicine. J. Physiol. 2002; 542:3–16. [PubMed: 12096044]

Aharon R, Bar-Shavit Z. Involvement of aquaporin 9 in osteoclast differentiation. J. Biol. Chem. 2006; 281:19305–19309. [PubMed: 16698796]

Bai S, Kitaura H, Zhao H, Chen J, Muller JM, Schule R, Darnay B, Novack DV, Ross FP, Teitelbaum SL. FHL2 inhibits the activated osteoclast in a TRAF6-dependent manner. J. Clin. Invest. 2005; 115:2742–2751. [PubMed: 16184196]

Baron R, Neff L, Louvard D, Courtoy PJ. Cell-mediated extracellular acidification and bone resorption: evidence for a low pH in resorbing lacunae and localization of a 100-kD lysosomal membrane protein at the osteoclast ruffled border. J. Cell. Biol. 1985; 101:2210–2222. [PubMed: 3905822]

Carbrey JM, Gorelick-Feldman DA, Kozono D, Praetorius J, Nielsen S, Agre P. Aquaglyceroporin AQP9: solute permeation and metabolic control of expression in liver. Proc. Natl. Acad. Sci. U S A. 2003; 100:2945–2950. [PubMed: 12594337]

Drake FH, Dodds RA, James IE, Connor JR, Debouck C, Richardson S, Lee-Rykaczewski E, Coleman L, Rieman D, Barthlow R, Hastings G, Gowen M. Cathepsin K, but not cathepsins B, L, or S, is abundantly expressed in human osteoclasts. J. Biol. Chem. 1996; 271:12511–12516. [PubMed: 8647859]

Elkjaer M, Vajda Z, Nejsum LN, Kwon T, Jensen UB, Amiry-Moghaddam M, Frokiaer J, Nielsen S. Immunolocalization of AQP9 in liver, epididymis, testis, spleen, and brain. Biochem. Biophys. Res. Commun. 2000; 276:1118–1128. [PubMed: 11027599]

Fan HT, Morishima S, Kida H, Okada Y. Phloretin differentially inhibits volume-sensitive and cyclic AMP-activated, but not Ca-activated, Cl(-) channels. Br. J. Pharmacol. 2001; 133:1096–1106. [PubMed: 11487521]

Hotokezaka H, Sakai E, Kanaoka K, Saito K, Matsuo K, Kitaura H, Yoshida N, Nakayama K. U0126 and PD98059, specific inhibitors of MEK, accelerate differentiation of RAW264.7 cells into osteoclast-like cells. J. Biol. Chem. 2002; 277:47366–47372. [PubMed: 12237315]

Ishibashi K, Kuwahara M, Gu Y, Tanaka Y, Marumo F, Sasaki S. Cloning and functional expression of a new aquaporin (AQP9) abundantly expressed in the peripheral leukocytes permeable to water

and urea, but not to glycerol. Biochem. Biophys. Res. Commun. 1998; 244:268–274. [PubMed: 9514918]

Knepper MA, Star RA. The vasopressin-regulated urea transporter in renal inner medullary collecting duct. Am. J. Physiol. 1990; 259:F393–401. [PubMed: 2204274]

Kuriyama H, Shimomura I, Kishida K, Kondo H, Furuyama N, Nishizawa H, Maeda N, Matsuda M, Nagaretani H, Kihara S, Nakamura T, Tochino Y, Funahashi T, Matsuzawa Y. Coordinated regulation of fat-specific and liver-specific glycerol channels, aquaporin adipose and aquaporin 9. Diabetes. 2002; 51:2915–2921. [PubMed: 12351427]

Lacey DL, Timms E, Tan HL, Kelley MJ, Dunstan CR, Burgess T, Elliott R, Colombero A, Elliott G, Scully S, Hsu H, Sullivan J, Hawkins N, Davy E, Capparelli C, Eli A, Qian YX, Kaufman S, Sarosi I, Shalhoub V, Senaldi G, Guo J, Delaney J, Boyle WJ. Osteoprotegerin ligand is a cytokine that regulates osteoclast differentiation and activation. Cell. 1998; 93:165–176. [PubMed: 9568710]

Liu Y, Promeneur D, Rojek A, Kumar N, Frokiaer J, Nielsen S, King LS, Agre P, Carbrey JM. Aquaporin 9 is the major pathway for glycerol uptake by mouse erythrocytes, with implications for malarial virulence. Proc. Natl. Acad. Sci. U S A. 2007; 104:12560–12564. [PubMed: 17636116]

Nesbitt SA, Horton MA. Trafficking of matrix collagens through bone-resorbing osteoclasts. Science. 1997; 276:266–269. [PubMed: 9092478]

Rojek AM, Skowronski MT, Fuchtbauer EM, Fuchtbauer AC, Fenton RA, Agre P, Frokiaer J, Nielsen S. Defective glycerol metabolism in aquaporin 9 (AQP9) knockout mice. Proc. Natl. Acad. Sci. U S A. 2007; 104:3609–3614. [PubMed: 17360690]

Smith BL, Preston GM, Spring FA, Anstee DJ, Agre P. Human red cell aquaporin CHIP. I. Molecular characterization of ABH and Colton blood group antigens. J. Clin. Invest. 1994; 94:1043–1049. [PubMed: 7521882]

Teitelbaum SL. Bone resorption by osteoclasts. Science. 2000; 289:1504–1508. [PubMed: 10968780]

Tsukaguchi H, Shayakul C, Berger UV, Mackenzie B, Devidas S, Guggino WB, van Hoek AN, Hediger MA. Molecular characterization of a broad selectivity neutral solute channel. J. Biol. Chem. 1998; 273:24737–24743. [PubMed: 9733774]

Udagawa N, Takahashi N, Akatsu T, Tanaka H, Sasaki T, Nishihara T, Koga T, Martin TJ, Suda T. Origin of osteoclasts: mature monocytes and macrophages are capable of differentiating into osteoclasts under a suitable microenvironment prepared by bone marrow-derived stromal cells. Proc. Natl. Acad. Sci. U S A. 1990; 87:7260–7264. [PubMed: 2169622]

Vignery A. Osteoclasts and giant cells: macrophage-macrophage fusion mechanism. Int. J. Exp. Pathol. 2000; 81:291–304. [PubMed: 11168677]

Wang L, Liu S, Quarles LD, Spurney RF. Targeted overexpression of G protein-coupled receptor kinase-2 in osteoblasts promotes bone loss. Am. J. Physiol. Endocrinol. Metab. 2005; 288:E826–834. [PubMed: 15585587]

Yamaguchi S, Ishikawa T. Electrophysiological characterization of native Na+-HCO3-cotransporter current in bovine parotid acinar cells. J. Physiol. 2005; 568:181–197. [PubMed: 16037094]

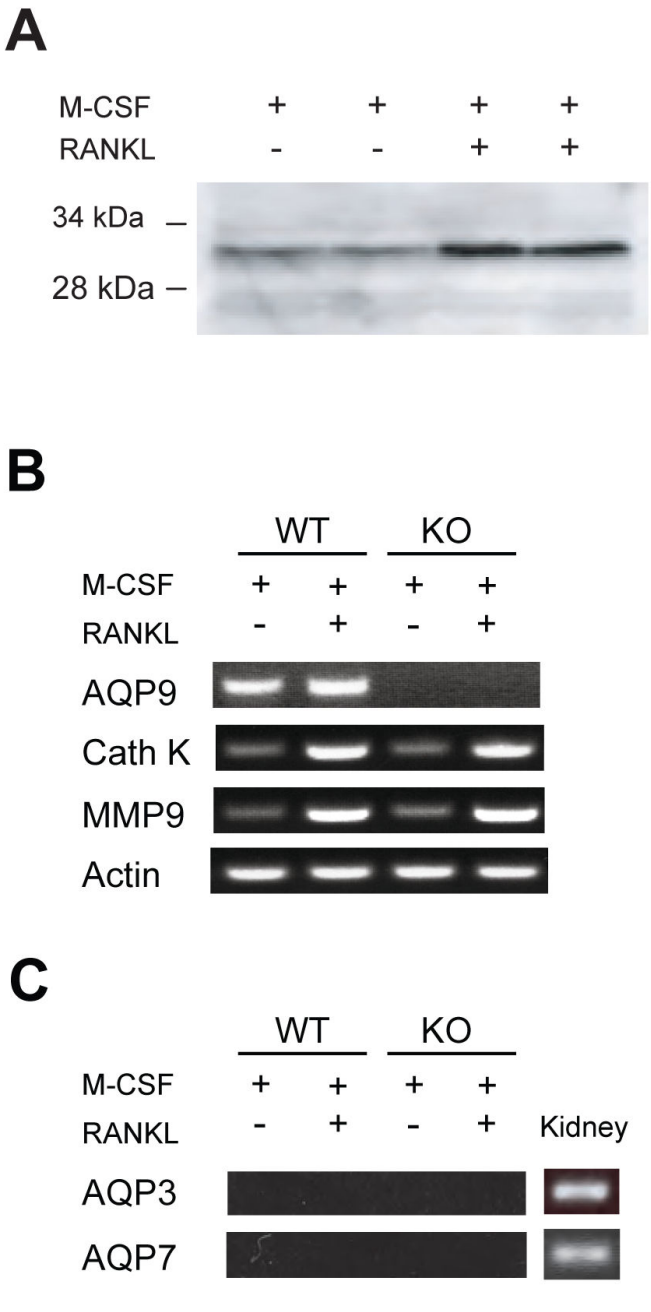

Fig. 1. Expression of AQP9 during osteoclast differentiation

A. Expression of AQP9 detected by Western blot in RAW264.7 cells and osteoclasts differentiated from RAW264.7 cells in the presence of 10 ng/ml M-CSF and 50 ng/ml RANKL. Samples were loaded as duplicates.

B. Confirmation of AQP9 expression in osteoclasts with AQP9 null mice. BMMs from wild type (WT) and AQP9 null mice (KO) were isolated and differentiated into osteoclasts in the presence of 10 ng/ml M-CSF and 100 ng/ml RANKL. The expression of AQP9 and osteoclast markers (MMP9 and Cath K) in BMMs (with M-CSF) and BMM-derived

osteoclasts (with M-CSF and RANKL) isolated from wild type and AQP9 null mice was analyzed by RT-PCR. Increased expression of MMP9 and Cathepsin K is a characteristic of osteoclasts. Amplification of β-actin was used as a sample loading control.

C. AQP3 and AQP7 expression in BMM-derived osteoclasts from AQP9 null mice. BMMs from wild type (WT) and AQP9 null mice (KO) were isolated and differentiated into osteoclasts in the presence of 10 ng/ml M-CSF and 100 ng/ml RANKL. The expression of AQP3 and AQP7 in BMMs (with M-CSF) and BMM-derived osteoclasts (with M-CSF and RANKL) isolated from wild type and AQP9 null mice was analyzed by RT-PCR. Amplification of AQP3 and AQP7 from mouse kidney was used as a positive control.

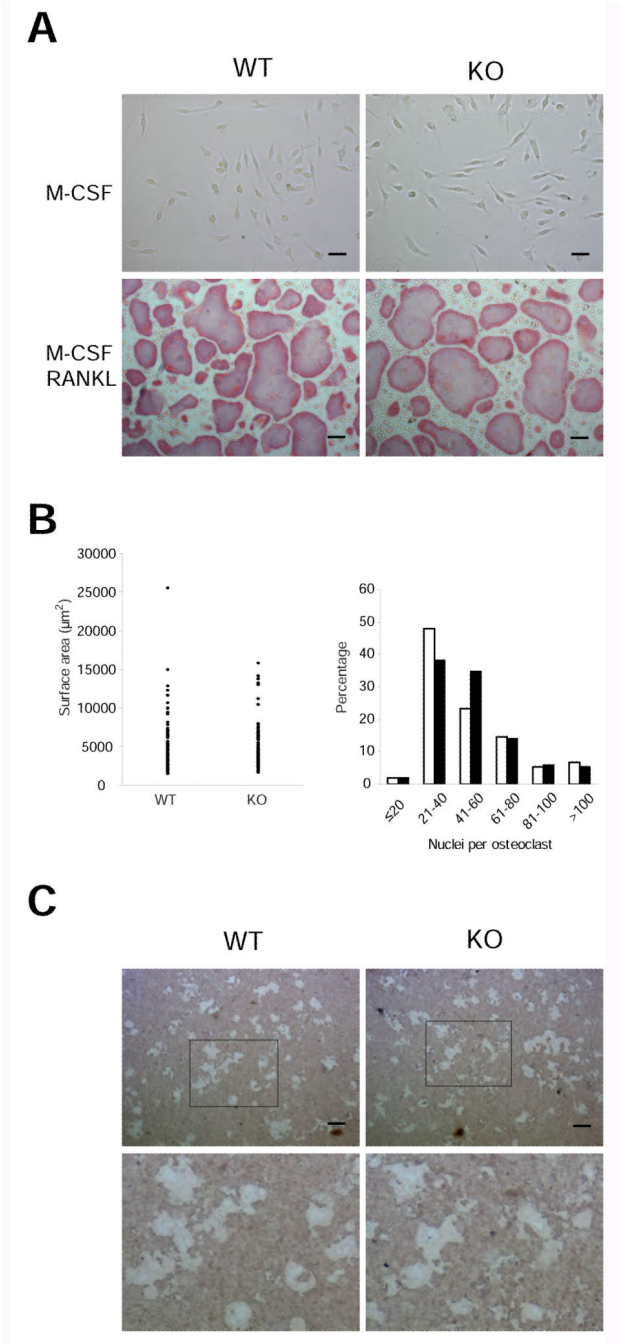

Fig. 2. Differentiation of AQP9 null BMMs into osteoclasts

A. Morphology of BMMs (with M-CSF) and BMM-derived osteoclasts (with M-CSF and RANKL) from wild type (WT) and AQP9 null (KO) mice analyzed by TRAP staining. Spread and nonspread TRAP positive osteoclasts are shown. Bars, 100 μm.

B. Distribution and range of surface area (left) and nuclear number (right) of spread BMM-derived osteoclasts from wild type (WT) and AQP9 null (KO) mice (osteoclasts counted per mouse=50, n=3). In the right panel: WT, open bars; KO, closed bars.

C. Functional activity of osteoclasts derived from BMMs from wild type (WT) and AQP9 null (KO) mice analyzed by bone resorption assay. BMMs were seeded and differentiated into osteoclasts on the BD BioCoat Osteologic Bone Cell Culture System. Upper panels: Absorption pits formed by osteoclasts were shown as pale spots. Lower panels: Higher-magnification view of boxed area in upper panels. Bars, 100 μm.

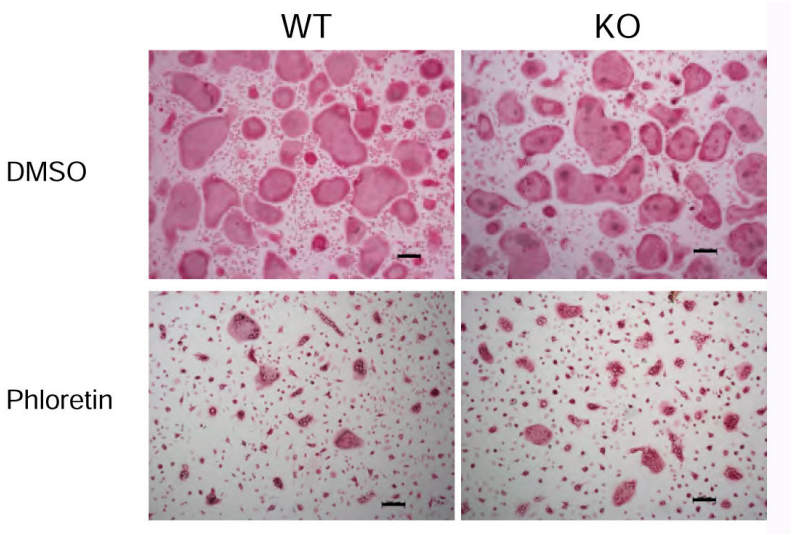

Fig. 3. Effect of phloretin on osteoclast differention

Osteoclasts differentiated from wild type (WT) and AQP9 null (KO) BMMs were incubated with DMSO or 50 μM phloretin for the final two days of differentiation with M-CSF and RANKL. All samples were stained to show TRAP-positive BMM-derived osteoclasts. Bars, 100 μm.

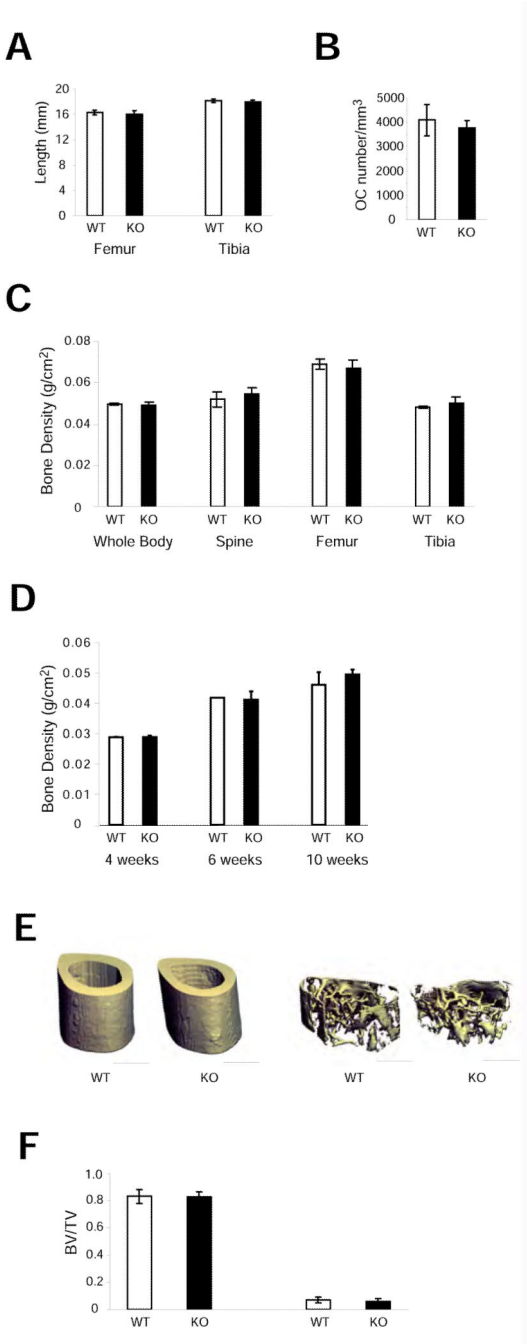

Fig. 4. Phenotypic analyses of bones from AQP9 null mice

A. Length of tibias and femurs of wild type (WT, n=7) and AQP9 null mice (KO, n=7).

B. Number of osteoclasts in the cortical area adjacent to the growth plate of tibias from wild type (WT; slides counted=5, n=3) and AQP9 null mice (KO; slides counted=5, n=3).

C. Bone density of whole bodies, spines, femurs, and tibias from adult wild type (WT, n=5) and AQP9 null mice (KO, n=5) analyzed by DEXA.

D. Bone density of whole bodies from 4, 6, and 10 week old wild type (WT, n=2) and AQP9 null mice (KO, n=2) analyzed by DEXA.

E. Structure of cortical area (left side) and trabecular area (right side) of femurs from wild type (WT, n=7) and AQP9 null mice (KO, n=7) after 3-D reconstruction by μCT. Bars, 0.5 mm.

F. Quantitative analysis of the ratio of bone volume versus tissue volume (BV/TV) of femurs from wild type (WT, n=7) and AQP9 null mice (KO, n=7) to determine the bone density of femurs by μCT.